Structure and Ethanol Complexation of Cyclic Tetrasaccharide in Aqueous Solution Studied by NMR and Molecular Mechanics

Noriaki FUNASAKI,*[,a] Seiji ISHIKAWA,[a] Shun HIROTA,[a] Saburo NEYA,[b] and Tomoyuki NISHIMOTO[c]

[a] *Kyoto Pharmaceutical University; Misasagi, Yamashina-ku, Kyoto 607–8414, Japan:* [b] *Graduate School of Pharmaceutical Sciences, Chiba University; Inage-Yayoi, Chiba 263–8522, Japan: and* [c] *Hayashibara Biochemical Laboratories Inc.; Amaseminami-machi, Okayama 700–0834, Japan.*

Received January 8, 2004; accepted March 25, 2004; published online March 26, 2004

The structure and ethanol complexation of a cyclic tetrasaccharide (CTS) in aqueous solution were investigated by proton NMR spectroscopy and molecular mechanics calculations. Two glucose units, A and B, of CTS are alternatively bonded by α-1,3 and α-1,6 linkages. The overlapped signals of protons A5, A6*S*, A6*R*, B3, B6*S* and B6*R* were resolved by spectral simulations to determine their chemical shifts and vicinal coupling constants. All vicinal coupling constants except for the A5–A6 spin system are consistent with the dihedral angles in the X-ray crystal structure. Each of protons A5, A6*S*, and A6*R* in the two units of A is equivalent with respect to the chemical shift. The vicinal coupling constants of $^3J_{5-6S}$ and $^3J_{5-6R}$ for unit A are close to the average of two rotamers that are present in crystals. The intensities of cross-peaks in the rotating frame nuclear Overhauser effect spectroscopy (ROESY) spectrum were rather well correlated with the effective distances calculated for the X-ray structure and molecular mechanics structures calculated *in vacuo* and water, although they are slightly better correlated with molecular mechanics structure *in vacuo* than with the other structures. From the changes of the chemical shifts of several CTS protons with increasing ethanol concentration, it was suggested that adsorption sites of ethanol on the plate structure of CTS are protons B2 and B4 (site B) in the concave face side and protons A1 and A2 (site A) in the convex back side. The binding constants for sites A and B are 0.0061 and 0.0176 M^{-1}, respectively. These binding constants are much smaller than a value of 4.1 M^{-1} for the ethanol–α-cyclodextrin complex.

Key words cyclic tetrasaccharide; NMR; ethanol binding; solution structure; molecular mechanics

Relatively few examples are known of cyclic oligosaccharides, the best known being cyclodextrin.[1,2] Other cyclic oligosaccharides have been prepared by means of enzymes and chemical syntheses.[3—6]

Cyclo-[→6]-α-D-glucopyranosyl-(1→3)-α-D-glucopyranosyl-(1→6)-α-D-glucopyranosyl-(1→3)-α-D-glucopyranosyl-(1→), a cyclic tetrasaccharide (CTS), is prepared by enzymic hydrolysis of the polysaccharide alternan.[3] Recently, CTS has also been synthesized by glycosyltransferase.[6] This tetrasaccharide attracts increased interest due to relative resistance to microbial and enzymic degradation. Most of the signals in proton and carbon NMR spectra were assigned.[3] The structure of CTS was determined by X-ray analysis of single crystals and molecular dynamics simulations: CTS has a plate shape.[7]

Cyclodextrins can entrap many compounds in their cavities. As a result, cyclodextrin is an interesting host compound from the academic viewpoint and is applied in chemicals, pharmaceuticals and foods industries.[1,2,8—14] Cyclogentiotetraose peracetate, a cyclic tetrasaccharide, can bind alkali cations in organic solvents.[15] The ability of CTS to bind metal cations in aqueous solutions has very recently been investigated.[16] To our knowledge, there is no report on the affinity of CTS (Fig. 1) to organic compounds.

In the present work, we aimed to estimate the three-dimensional structure of CTS in aqueous solution by proton NMR and molecular mechanics calculations as well as the inclusion property of CTS. The assignment of H6*S* and H6*R* was established by spectral simulations and the vicinal spin–spin coupling constants $^3J_{5-6S}$ and $^3J_{5-6R}$ were determined. These data revealed a clear difference in the internal rotation of the C5–C6 bond between the crystal and solution structures. The rotating frame nuclear Overhauser effect spectroscopy (ROESY) spectrum of CTS was compared with the crystal structure and the structures predicted by molecular mechanics in the presence and absence of water. Because the cavity of CTS is very small, large organic compounds will be not accommodated therein. Therefore we chose ethanol, a relatively small organic molecule and investigated complex formation between it and CTS on the basis of chemical shift data.

Experimental

Materials The used specimen of CTS·5H_2O was 99.97% pure.[6] Commercial samples of tetramethylammonium chloride (Nacalai Tesque Co.), ethanol (Wako Pure Chemicals Co.), and 99.9 atom% deuterium oxide (Aldrich) were used.

NMR Measurements All proton NMR experiments were carried out in deuterium oxide at 298.2±0.1 K. The spectra were recorded on a JEOL Lambda 500 spectrometer. The proton chemical shift and spin–spin coupling constant were determined by Nuts data processing software (Acorn NMR Inc.). The chemical shift of 1 mmol dm^{-3} (mM) tetramethylammonium chloride at 3.176 ppm was used as the internal standard.[13,14] Chemical shifts of CTS protons in 10.8 mM CTS solution were determined as a function of the ethanol concentration.

Two-dimensional ROESY of a 20 mM CTS solution was performed at 500 MHz with the JEOL standard pulse sequences; data consisted of 8 transients collected over 2048 complex points. A mixing time of 250 ms, a repetition delay of 1.2 s and a 90° pulse width of 11.0 μs were used. The ROESY data set was processed by applying an exponential function in both dimensions and zero-filling to 2048×2048 real data points prior to the Fourier transformation. Small cross-peaks were neglected, because their magnitude was close to that of noise. The volume of a ROESY cross-peak was calculated by summation of spectrum intensities with a certain region around the cross-peak and it slightly depended on the region of integration, peak overlap, and the signal-to-noise ratio.

Molecular Mechanics Calculations Molecular mechanics calculations of CTS were performed with the Molecular Simulation Insight II/Discover III (2000) on a Silicon Graphics Octane workstation. The Discover III CVFF

* To whom correspondence should be addressed. e-mail: funasaki@mb.kyoto-phu.ac.jp

force field was used for energy minimization. These calculations were performed in the presence and absence of water. The partial atomic charges and the structure of CTS *in vacuo* were obtained by optimization using the Discover III module of Insight II, and potential types were derived from the CVFF force field. The periodic boundary condition was applied on a cubic cell in which CTS was centered. The optimized structure of CTS was then soaked in a 2 nm layer of water (975 water molecules per CTS molecule) and the total potential energy of this system was minimized. Energy minimization was performed using the conjugate gradients method to a derivative of 0.001 kcal mol^{-1} with Insight II′ default values (van der Waals' cut off distance=0.95 nm and electrostatic cut off distance=0.95 nm). The optimized structure of CTS *in vacuo* (in the absence of water) was also determined.

Results

One-Dimensional NMR Spectrum The chemical structure of CTS is shown in Fig. 1. CTS consists of two kinds of glucose units (units A and B) that are linked at two positions, α-1 (unit A)–6 (unit B) and α-3 (unit A)–1 (unit B). Figure 2 shows a partial one-dimensional NMR spectrum in the region of δ=3.7 to 3.9 ppm, where the signals of protons A6*R*, B6*R*, B3, A5 and A6*S* overlap with one another. To resolve these overlapping signals, we simulated this spectrum using the best fit values of chemical shifts, vicinal spin–spin coupling constants, and a single half-width. The simulated (dashed line) spectrum is close to the observed one (solid line). Minor differences in protons B3 and B6*R* resulted from the assumption of a single half-width. Actually, the half-width will depend on the kinds of proton. The chemical shifts were obtained as follows: δ(A6*R*)=3.753, δ(B6*R*)=3.759, δ(B6*S*)=3.767, δ(B3)=3.775, δ(A5)=3.796 and δ(A6*S*)=3.829 ppm. The chemical shifts of the other protons are close to the literature values.[3] Although each unit of A and B has two protons, their chemical shifts are equivalent. This finding indicates that the internal motion of CTS is rapid on the NMR time scale.

The vicinal coupling constants (^3J) for all pairs of protons are given in Table 1, together with the dihedral angles in crystals.[7] The dihedral angles for two A5–A6*R* pairs in the crystals are very distant from each other, although those for the other pairs are close to each other. The vicinal coupling constants for all pairs except for the A5–A6*R* pair are consistent with their dihedral angles in the crystals.

The two A5–A6*R* pairs in the crystals are nonequivalent, *viz*., in the trans (*t*) and gauche (*g*) conformation around the C5–C6 bond. For unit A we can presume that three rotamers different in the dihedral angle around the C5–C6 bond may be present, as shown in Fig. 3. In crystals, one of the two A units is in the *gt* conformer and the other is in the *gg* conformer. Each of protons A5 and A6*R* has a single chemical shift and the vicinal coupling constants for the A5–A6*R* and A5–A6*S* spin systems have different values. For unit B the internal rotation angle around the C5–C6 axis in aqueous solution is close to that in crystals: the vicinal coupling constants for the trans and gauche conformations are 9.9 and 2.0 Hz for the B5–B6*R* and B5–B6*S* pairs (Table 1), respectively. These vicinal coupling constants will be used for unit A. If unit A consists of a 1 : 1 mixture of the *gt* and *gg* conformers, the vicinal coupling constants of $^3J_{\mathrm{A5–A6}S}$ and $^3J\mathrm{A}_{\mathrm{5–A6}R}$ are predicted to be 2.0 and 6.0 Hz, respectively. These calculated values are close to the observed ones. If unit A consists of a 1 : 1 : 1 mixture of the *gt*, and *gg*, and *tg* conformers, the vicinal coupling constants of $^3J_{\mathrm{A5–A6}S}$ and $^3J_{\mathrm{A5–A6}R}$ are predicted to be both 4.7 Hz: the C5–C6 bond does not rotate freely. Therefore, the C5–C6 bond for unit A in aqueous solution rapidly interchanges between the *gt* and *gg* conformers. This is the major difference between the structures in crystals and aqueous solution.

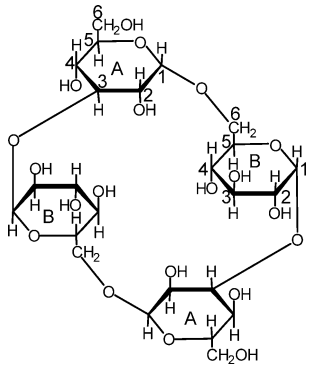

Fig. 1. Structure of CTS and Labeling of Carbons

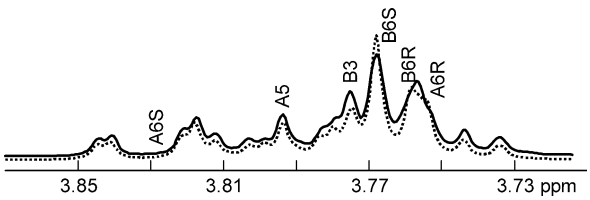

Fig. 2. Partial Observed (Solid Line) and Simulated (Dashed Line) Proton NMR Spectra of a 20 mM CTS Solution

The baseline of the solid line is moved slightly upward for clarity.

Table 1. Vicinal Spin–Spin Coupling Constants ^3J and Crystal Dihedral Angles θ of CTS[a]

Pair	^3J (Hz)	θ (degree)
A1–A2	3.6	58.3, 54.5
A2–A3	9.8	−178.7, −178.5
A3–A4	9.0	−176.7, −179.5
A4–A5	9.7	−172.7, −179.7
A5–A6*S*	2.2	64.7, 70.5
A5–A6*R*	5.2	175.6, 50.4
B1–B2	3.8	55.9, 54.1
B2–B3	9.7	−174.8, −175.2
B3–B4	9.1	173.8, 172.5
B4–B5	10.2	−175.6, −174.8
B5–B6*S*	2.0	59.0, 59.2
B5–B6*R*	9.9	179.0, 179.8

a) Crystal data taken from ref. 7.

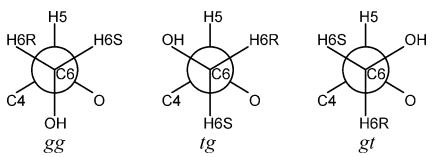

Fig. 3. Newman Projections of Three Rotamers around the C5–C6 Bond for Unit A: (a) *gt* Conformer, (b) *tg* Conformer and (c) *gg* Conformer

ROESY Spectrum The intensity of a cross-peak in the ROESY spectrum of a 20 mM CTS solution was determined by integration of the peak. The intensity is proportional to the number N of equivalent protons. Because the signals of B6*R* and B6*S* overlapped with each other, they were regarded

Table 2. Cross-Peak Intensities between Pairs of Protons in the ROESY Spectrum

Pair	*ROE*/*N*	Pair	*ROE*/*N*
A3B1	211	B1B2	415
A1B6	159	B2B4	262
B4B6	124	A1B5	49
A3B5	123	A2B5	11
B1B5	6	A4B1	41
B2B5	19	A5A6B1B3B6[a)]	39
A2B1	26		

a) Although the cross peaks consist of five overlapping signals, they were treated as a single cross peak.

as being equivalent protons. Some of protons B3, A5, A6*R*, A6*S*, B6*R* and B6*S* have cross-peaks with proton B1. They were regarded as 12 equivalent protons, because they could not be resolved. The observed ROE intensity is given in Table 2.

When internal rotations of CTS are slower than the overall tumbling, we can write the ROE intensity as[17,18)]

$$ROE/N = k d_{\mathrm{eff}}^{-6} \quad (1)$$

Here the effective distance, d_{eff}, is defined as[17,18)]

$$(d_{\mathrm{eff}})^{-6} = (1/N)\sum_{i,j} d_{ij}^{-6} \quad (2)$$

Here N stands for the product of the numbers of equivalent protons in the groups corresponding to protons i and j. The values for *ROE*/*N* are given in Table 2. The d_{eff} values for the corresponding pairs were calculated on the basis of the crystal structure of CTS.[7)] The plots of *ROE*/*N* *versus* d_{eff} are shown by circles in Fig. 4.

Molecular Mechanics Calculations To seek better structures of CTS, we estimated the energy-optimized structures in aqueous solution and *in vacuo* by molecular mechanics calculations. The effective distances for these solution and vacuum structures were calculated and are plotted against the observed ROE intesities in Fig. 4. All of the d_{eff} values calculated for these structures are smaller than 0.5 nm. An ROE cross-peak between a pair of protons closer than this distance is usually observed.[9)]

A superimposition of the crystal, solution, and vacuum structures is shown in Fig. 5. These three structures are similar to one another.

Complex Formation between CTS and Ethanol The effect of ethanol on the one-dimensional NMR spectrum of 5 mM CTS was investigated. At low ethanol concentrations, a single signal of HDO, the hydroxyl proton of ethanol and hydroxyl protons of CTS appeared around δ=4.8 ppm. This finding indicates that a rapid exchange occurs among these protons. This signal moved to a lower field with increasing ethanol concentration. Above 0.78 M, a separate broad signal appeared. As the ethanol concentration was increased, this signal moved to 5.5 ppm and the signal due to HDO and CTS moved to a higher field. The broad separate signal is also observed for concentrated ethanol solutions (above C_{EtOH}=0.78 M) in water without CTS, because the exchange between HDO and the hydroxyl proton of ethanol is slow.[19)]

The chemical shifts of most of the CTS protons moved to a high field with increasing ethanol concentration. The chemical shift changes for A1, A2, A3 A4, B1, B2, B4 and B5 are shown as a function of ethanol concentration in Fig. 6. Because the signals of the other protons were overlapped with each other, the chemical shifts of these protons were not determined as a function of ethanol concentration.

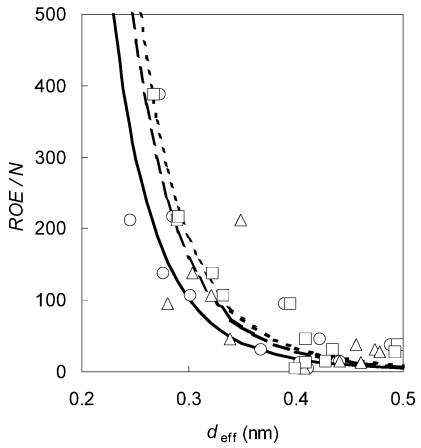

Fig. 4. Correlations between the ROESY Intensity and the Effective Distance for the Crystal (Circles), Solution (Triangles) and Vacuum (Squares) Structures

The solid, dashed and dotted lines for the crystal, solution and vacuum structures, respectively, were calculated from Eq. 1.

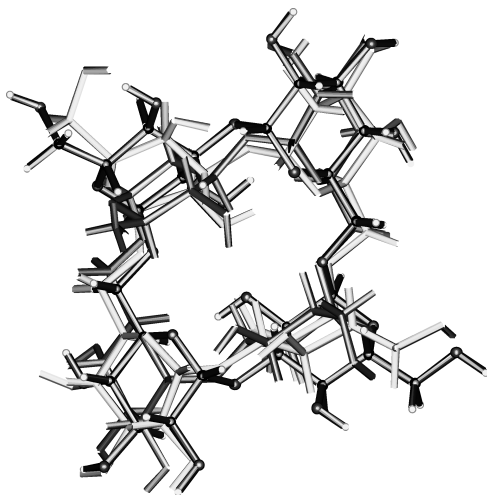

Fig. 5. Superimposition of the Crystal (in Black), Solution (in Dark Gray) and Vacuum (in Light Gray) Structures of CTS

1 : 1 Complex Model When CTS and ethanol form the 1 : 1 complex (CTS·ET), the observed chemical shift of any CTS proton will be written as

$$\begin{aligned}\delta &= \{[\mathrm{CTS}]\delta_{\mathrm{CTS}} + [\mathrm{CTS\cdot ET}]\delta_{\mathrm{CTS\cdot ET}}\}/C_{\mathrm{CTS}} \\ &= \{[\mathrm{CTS}]\delta_{\mathrm{CTS}} = K[\mathrm{CTS}][\mathrm{ET}]\delta_{\mathrm{CTS\cdot ET}}\}/C_{\mathrm{CTS}}\end{aligned} \quad (3)$$

Here, [CTS], [CTS·ET], and [ET] stand for the free-CTS concentration, the bound CTS concentration, and the free-ethanol concentration, respectively. δ_{CTS} and $\delta_{\mathrm{CTS\cdot ET}}$ denote the chemical shifts of free and bound CTS species, C_{CTS} is the total concentration and K is the 1 : 1 binding constant.

Using all chemical shift data shown in Fig. 6, we determined the binding constant and the chemical shift variations at full binding ($\Delta\delta = \delta_{\mathrm{CTS\cdot ET}} - \delta_{\mathrm{CTS}}$); $K = 0.010 \pm 0.002\ \mathrm{M}^{-1}$, $\Delta\delta$(A1) = −0.666, $\Delta\delta$(A2) = −0.495, $\Delta\delta$(A3) = −0.052, $\Delta\delta$(A4) = −0.389, $\Delta\delta$(B1) = −0.388, $\Delta\delta$(B2) = −0.756, $\Delta\delta$(B4) = −0.756 and $\Delta\delta$(B5) = 0.017 ppm. This binding

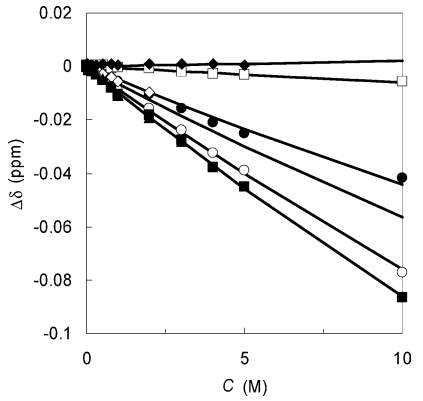

Fig. 6. Chemical Shift Variations of Eight CTS Protons as a Function of Ethanol Concentration: A1 (Open Circles), A2 (Open Rhombuses), B1 (Closed Circles), B2 (Closed Triangles), B4 (Closed Squares) and B5 (Closed Rhombuses)

The solid lines were calculated by Eqs. 12—16 with the best fit values of K_A, K_B, $\Delta\delta$(A) and $\Delta\delta$(B) given in the text. The chemical shifts of protons A2, A4 and B2 at higher concentrations than 1.2 M could not be determined because of overlapping with other signals.

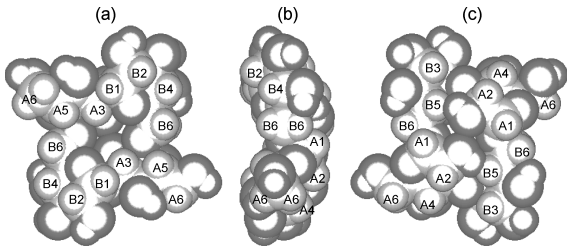

Fig. 7. (a) The Concave Face, (b) the Side with the Face in Left and the Back in Right, and (c) the Convex Back of CTS

The hydrophobic CH and CH_2 groups are shown in light gray and the hydrophilic OH and O groups are shown in dark gray. Ethanol would be adsorbed on protons B2 and B4 and on protons A1 and A2.

constant is much smaller than that for the α-cyclodextrin–ethanol complex (4.1 M^{-1}).[20]

From the magnitude of chemical shift variations, binding sites may be inferred. Protons B2 and B4 are on the concave face of the plate of CTS and are close to each other. Because the chemical shifts for these protons are varied largely, this will be a first binding site. The chemical shift variation of proton A3 is small probably because it is in the interior of the plate. Protons A1 and A2 are on the back of CTS and are close to each other. These protons would form the second binding site. These binding sites are close to the surfaces of the concave face and the convex back of CTS, as shown in Fig. 7. Ethanol would be adsorbed, instead of bound, on protons B2 and B4 and on protons A1 and A2.

The chemical shifts of the methyl and methylene protons of ethanol exhibit small and biphasic variations with increasing ethanol concentration. At low concentrations (below C_{EtOH}=0.78 M) the exchange between the hydroxyl proton and the deuterium atom of deuterium oxide is rapid, whereas at higher concentrations it is slow. Therefore, the increase in ethanol concentration results in a decrease of CH_3CH_2OH and an increase of CH_3CH_2OD. This is the reason for the biphasic variations in the chemical shifts of ethanol protons. Thus, it was difficult to determine the chemical shift variations of the ethanol protons and hence to estimate which proton of ethanol is adsorbed on CTA. Then, it is not natural that an ethanol molecule is adsorbed on one side of CTS to cause large shifts of protons on the both sides of CTS. Therefore, this structural difficulty rules out the 1 : 1 model.

Four Independent Binding Site Model As shown in Fig. 6, the A1 and A2 protons exhibit large variations and they are close to each other at the convex side. They can form a binding site (site A) to ethanol. There are two A sites. The B2 and B4 protons exhibit large variations and they are close to each other at the concave side. This is named site B. There are two B sites. Therefore, CTS has four binding sites to ethanol. The complex that has i ethanol molecules at the site A and j ethanol molecules at the site will be denoted as $CTSA_iB_j$, where i and j, respectively, are 0, 1, and 2. This complex can be formed stepwise as[21,22]

$$CTSA_{i-1}B_j + ET = CTSA_iB_j \tag{4}$$

and

$$CTSA_iB_{j-1} + ET = CTSA_iB_j \tag{5}$$

The equilibrium constants of these reactions are defined as

$$K_A = [CTSA_iB_j]/[CTSA_{i-1}B_j][ET] \tag{6}$$

and

$$K_B = [CTSA_iB_j]/[CTSA_iB_{j-1}][ET] \tag{7}$$

If these reactions occur independently, we can expect that K_A and K_B are independent of i and j. Then, the concentration of complex $CTSA_iB_j$ can be written as

$$[CTSA_iB_j] = n_{ij}K_A^iK_B^j[CTS][ET]^{i+j} \tag{8}$$

$$n_{ij} = \{2!/(2-i)!\} \times \{2!/(2-j)!\} \tag{9}$$

The total concentration of CTS can be written as

$$C_{CTS} = \sum_0^2\sum_0^2 [CTSA_iB_j] = [CTS]\sum_0^2\sum_0^2 n_{ij}K_A^iK_B^j[ET]^{i+j} \tag{10}$$

The total concentration of ethanol can be written as

$$C_{ET} = [ET] + \sum_0^2\sum_0^2 [CTSA_iB_j] = [ET] + [CTS]\sum_0^2\sum_0^2 (i+j)n_{ij}K_A^iK_B^j[ET]^{i+j} \tag{11}$$

The chemical shift of a CTS proton can be written as

$$\delta = \sum_0^2\sum_0^2 [CTSA_iB_j]\delta_{CTSA_iB_j}/C_{CTS} = \sum_0^2\sum_0^2 n_{ij}K_A^iK_B^j[CTS][ET]^{i+j}\delta_{CTSA_iB_j}/C_{CTS} \tag{12}$$

If these complexations occur independently, regardless of i and j, we can assume the following equations:

$$\delta_{CTSA_1B_j} = \delta_{CTS} + \Delta\delta_A/2 \tag{13}$$

$$\delta_{CTSA_2B_j} = \delta_{CTS} + \Delta\delta_A \tag{14}$$

$$\delta_{CTSA_iB_1} = \delta_{CTS} + \Delta\delta_B/2 \tag{15}$$

$$\delta_{CTSA_iB_2} = \delta_{CTS} + \Delta\delta_B \tag{16}$$

In these equations, we took into consideration the effect of the average number of ethanol molecules bound to a binding site on the chemical shift.

If one regards K_A and K_B as two adjustable parameters, one can calculate theoretical concentrations of [CTS] and [ET] for a given set of C_{CTS} and C_{ET} from two simultaneous biquadratic equations, Eqs. 10 and 11. The biquadratic equations can be solved by the Newton–Raphson method.[23] Next, if one regards $\Delta\delta_A$ (or $\Delta\delta_B$) as an adjustable parameter, one can calculate a theoretical value for $\Delta\delta_A$ (or $\Delta\delta_B$) from Eqs. 12—14 (or Eqs. 12, 15, and 16) with the values of K_A, K_B, [CTS], and [ET]. These calculations are repeated to obtain the best fit values of K_A, K_B, and $\Delta\delta_A$ (or $\Delta\delta_B$) for the given set of C_{CTS} and C_{ET}. Furthermore, these calculations are made for all protons and all ethanol concentrations. Finally, one can obtain the best fit values of K_A, K_B, $\Delta\delta_A$, and $\Delta\delta_B$ to all observed chemical shifts. The chemical shifts of protons A1, A2, A3, A4, B1, B2, B4, and B5 were determined as a function of the ethanol concentration, as shown in Fig. 6. These chemical shift data were used to obtain the best fit values of $K_A=0.0061\,\text{M}^{-1}$, $K_B=0.0176\,\text{M}^{-1}$, $\Delta\delta(\text{A1})=-1.336$, $\Delta\delta(\text{A2})=-1.041$, $\Delta\delta(\text{A3})=-0.104$, $\Delta\delta(\text{A4})=-0.811$, $\Delta\delta(\text{B1})=-0.294$, $\Delta\delta(\text{B2})=-0.562$, $\Delta\delta(\text{B4})=-0.573$, $\Delta\delta(\text{B5})=-0.013$ ppm. The solid lines in Fig. 6 were calculated using these best fit values. The values of K_A and K_B are much smaller than the 1 : 1 binding constant ($4.1\,\text{M}^{-1}$) between ethanol and α-cyclodextrin.[20]

Discussion

The present simulations of overlapped signals in the one-dimensional NMR spectrum allowed us to determine the chemical shifts and the vicinal spin–spin coupling constants of protons A5, A6*S*, A6*R*, B3, B6*S* and B6*R* (Fig. 2). The vicinal coupling constant data observed in aqueous solution are consistent with the dihedral angles for the crystal structure, except for protons A5, A6*S* and A6*R* (Table 1). In aqueous solution, protons A5, A6*S* and A6*R* in two A units become equivalent with each other by rapid interchanges between the *gt* and *gg* conformers (Fig. 3), so that the chemical shifts and each of the vicinal coupling constants are averaged over these conformers.

The ROESY intensity data are often classified qualitatively as "strong" and "weak". However, most polysaccharides have equivalent or indistinguishable protons in chemical shift. The ROESY intensity is proportional to the number of these protons. The qualitative expression of the ROESY intensity cannot take this multiplicity into consideration. The present quantitative analysis of the ROE intensity allows us to estimate the inter-proton distance more accurately than the qualitative expression.

However, the effects of spin-lock offset and TOCSY transfers or relays between J-coupled spins on the intensity of ROE cross-peaks must be taken into consideration to extract distance information.[17,18,24,25] For instance, the ROE intensity of the cross-peak between B1 and B2 may be influenced by vicinal spin–spin coupling as well as by the genuine ROE. TOCSY transfers or relays may also affect the intensities of cross-peaks between one of these protons and another proton. Keeping these limitations in mind, we cannot rigorously fit Eq. 1 to the observed ROE intensity data (Fig. 4).

Roughly speaking, the ROESY intensity data are consistent with any of the crystal, solution, and vacuum structures, because all effective distances calculated for these structures are smaller than 0.5 nm (Fig. 4).[9] The account of water in the molecular mechanics calculation results in slightly worse correlation: the effect of water on the molecular conformation remains unsolved. We have already suggested that hydration free energy can be estimated from the hydrophobic and hydrophilic molecular surface areas.[26] A cyclic trisaccharide in solution is shown to be the average over two conformational states.[27] Actually, a rapid exchange among numerous structures, including the above three structures, occurs and any single structure cannot explain the structure of CTS in aqueous solution. This will also hold true in the presence of ethanol. The NMR data provide the time-average structure. Molecular dynamics simulations can provide enormous structures as a function of time. These simulations were not carried out, because they would not much improve the agreement between theory and experiment.

The chemical shift is generally referred to an internal or external standard. These standards have merits and demerits.[12,13] The external standard has a demerit of difference in volume magnetic susceptibility between sample and reference.[13,14] In the present work the volume magnetic susceptibilities of deuterium oxide and ethanol are -0.705×10^{-6} and -0.594×10^{-6}, respectively.[13] Therefore, the volume magnetic susceptibility of sample changes from -0.705×10^{-6} toward -0.594×10^{-6}, as ethanol is added to deuterium oxide. This effect must be corrected to determine the true chemical shift.[13,14] On the other hand, the internal standard method has a demerit of intermolecular interactions between the standard and any component in solutions, and hence, the chemical shift of the standard may be changed. In the present work we chose tetramethylammonium chloride as an inert standard.[13]

Complex formation between CTS and ethanol was modeled by the 1 : 1 complex and the four complexes. However, the 1 : 1 complex model is inconsistent with large chemical shift variations of protons located at the concave and convex sides of CTS. Ethanol can be adsorbed on two kinds of sites, instead of binding to the central pocket of CTS. Two A1–A2 sites can bind two ethanol molecules by hydrophobic interactions (Fig. 7c). Two B2–B4 sites can also bind two ethanol molecules (Fig. 7a). Because these four binding sites are distant from one another, they will bind ethanol independently. Therefore, the four independent binding site model is better than the 1 : 1 complex model.

The present result indicates that CTS binds ethanol weakly on the concave and convex sides, instead of the central small pocket. From this result it is suggested that CTS has a weak binding capacity for most organic compounds. The central pocket of CTS can bind small inorganic ions.[15,16] Because CTS and its derivatives have high aqueous solubility and low toxicity, they could be added in foods and pharmaceuticals to remove toxic metal cations (Pb^{2+}, Ag^{+}, and other ions) and to keep useful cations (Ca^{2+}, Mg^{2+}, Fe^{3+}, and other ions).

Acknowledgements Thanks are due to Ms. Mika Minami and Ms. Tomoko Asada for some NMR measurements and analyses. The present work was supported by a Grant-in-Aid for the Frontier Research Program from the Ministry of Education, Culture, Sports, Science and Technology, Japan, which will be gratefully acknowledged.

References

1) Bender M. L., Komiyama M., "Cyclodextrin Chemistry," Chapters 2 and 3, Springer-Verlag, Berlin, 1978.
2) Szejtli J., "Cyclodextrin Technology," Chapters 2 and 3, Kluwer Academic Publishers, Dordrecht, The Netherlands, 1988.
3) Côte G. L., Biely P., *Eur. J. Biochem.*, **226**, 641—648 (1994).
4) Miller K. J., Gore R. S., Johnson R., Benesi A. J., Reinhold V. N., *J. Bacteriol.*, **172**, 136—142 (1990).
5) Gattuso G., Nepogodiev S. A., Stoddart J. F., *Chem. Rev.*, **98**, 1977—1996 (1998).
6) Nishimoto T., Aga H., Mukai K., Hashimoto T., Watanabe H., Kubota M., Fukuda S., Kurimoto M., Tsujisaka Y., *Biosci. Biotechnol. Biochem.*, **66**, 1806—1818 (2002).
7) Bradbrook G. M., Gessler K., Côte G. L., Momany F. A., Biely P., Bordet P., Perez S., Imberty A., *Carbohydr. Res.*, **329**, 655—665 (2000).
8) Križ Z., Koča J., Imberty A., Charlot A., Auzély-Velty R., *Org. Biomol. Chem.*, **1**, 2590—2595 (2003).
9) Schneider H.-J., Hacket F., Rüdiger V., Ikeda H., *Chem. Rev.*, **98**, 1755—1785 (1998).
10) Hedges A. R., *Chem. Rev.*, **98**, 2035—2044 (1998).
11) Funasaki N., Yamaguchi H., Ishikawa S., Neya S., *J. Phys. Chem. B*, **105**, 760—765 (2001).
12) Hada S., Neya S., Funasaki N., *J. Phys. Chem. B*, **103**, 2579—2584 (1999).
13) Funasaki N., Nomura M., Ishikawa S., Neya S., *J. Phys. Chem. B*, **105**, 7361—7365 (2001).
14) Funasaki N., Nomura M., Yamaguchi H., Ishikawa S., Neya S., *Bull. Chem. Soc. Jpn.*, **73**, 2727—2728 (2000).
15) Bonas G., Vignon M., *Rec. Trav. Chim. Pays-Bas*, **108**, 161—162 (1989).
16) Dunlap C. A., Côte G. L., Momany F. A., *Carbohydr. Res.*, **338**, 2367—2373 (2003).
17) Kessler H., Seip S., "Two-dimensional NMR Spectroscopy," 2nd ed., Chapter 5, ed. by Croasmun W. R., Carlson R. M. K., Wiley-VCH, New York, 1994.
18) Neuhaus D., Williamson M. P., "The Nuclear Overhauser Effect in Structural and Conformational Analysis," 2nd ed., Chapters 5, 9 and 12, Wiley-VCH, New York, 2000.
19) Glaros G., Cromwell N. H., *J. Chem. Educ.*, **48**, 202—203 (1971).
20) Gelb R. I., Schwartz L. M., Radeos M., Edmonds R. B., Laufer D. A., *J. Am. Chem. Soc.*, **104**, 6283—6288 (1982).
21) Barrow G. M., "Physical Chemistry for the Life Sciences," Chapter 6, McGraw-Hill, London, 1981.
22) Tanford C., "Physical Chemistry of Macromolecules," Chapter 8, John Wiley and Sons, New York, 1961.
23) Mortimer R. G., "Mathematics for Physical Chemistry," Chapter 9, Macmillan, New York, 1981.
24) Claridge T. D. W., "High-Resolution NMR Techniques in Organic Chemistry," Chapter 8, Pergamon, Oxford, 1999.
25) Hull W. E., "Two-dimensional NMR Spectroscopy," 2nd ed., Chapter 2, ed. by Croasmun W. R., Carlson R. M. K., Wiley-VCH, New York, 1994.
26) Funasaki N., Yamaguchi H., Ishikawa S., Neya S., *J. Phys. Chem. B*, **104**, 10412—10418 (2000).
27) Bonas G., Vignon M. R., Pérez S., *Carbohydr. Res.*, **211**, 191—205 (1991).